

Food Hydrocolloids

Interactions of cellulose cryogels and aerogels with water and oil: structure-function relationships --Manuscript Draft--

Manuscript Number:	
Article Type:	Research paper
Keywords:	porous materials; microstructure; adsorption; absorption; loading
Corresponding Author:	Stella Plazzotta University of Udine: Università degli Studi di Udine Udine, Udine ITALY
First Author:	Francesco Ciuffarin
Order of Authors:	Francesco Ciuffarin Marion Negrier Stella Plazzotta Michele Libralato Sonia Calligaris Tatiana Budtova Lara Manzocco
Abstract:	<p>Food-grade porous materials, aerogels and cryogels, were prepared from cellulose hydrogels obtained from solutions at increasing cellulose concentration (3, 4, 5%, w/w) by supercritical-CO₂-drying (SCD) and freeze-drying (FD), respectively. The structure depended on the applied drying technique, with aerogels showing a denser network with pores <200 nm in diameter, a specific surface area of 370-380 m²g⁻¹, and a porosity of 92-94%. Cryogels presented larger pores (2-5 μm diameter), much lower specific surface area (around 30 m²g⁻¹) and higher porosity (95-96%). Structuring cellulose into aerogels and cryogels increased its capability of interacting with water vapor. The absorption of water and oil was investigated as a function of time and at equilibrium. While water was almost immediately absorbed by both aerogels and cryogels, a much longer time was needed to reach oil absorption equilibrium. Moreover, aerogels required a longer time than cryogels. Material morphology governed absorption kinetics, while the absorption at equilibrium was directly dependent on material porosity rather than on its morphology or material-fluid affinity. As a result, due to their lower porosity, aerogels absorbed a lower amount of water or oil (4-8 gfluid/gdry matter) than cryogels (8-12 gfluid/gdry matter). All samples showed high fluid holding capacity (>96%); while water absorption caused a firmness decrease, the firmness of oil-filled materials was the same as of the unloaded ones. This study demonstrates that food-grade cellulose aerogels and cryogels can be structurally designed by acting on cellulose concentration and drying technique to obtain controlled food fluid loading.</p>
Suggested Reviewers:	Carlos Garcia Gonzalez carlos.garcia@usc.es Expert in bio-based aerogels Baldur Schroeter baldur.schroeter@tuhh.de Expert in aerogel characterization Dérick Rousseau rousseau@ryerson.ca Expert in food structure Kathirvel Ganesan k.ganesan@dlr.de Expert in porous materials

Dear Editor,

I would like to submit the manuscript entitled “*Interactions of cellulose cryogels and aerogels with water and oil: structure-function relationships*” by Francesco Ciuffarin, Marion Negrier, Stella Plazzotta, Michele Libralato, Sonia Calligaris, Tatiana Budtova, and Lara Manzocco for consideration for publication in *Food Hydrocolloids*.

The present study aimed to investigate the interaction between cellulose-based aerogels and cryogels with oil and water. To this purpose, cellulose hydrogels were prepared from cellulose solutions at increasing concentrations and dried via freeze drying or supercritical CO₂ drying. The derived food-grade aerogels and cryogels monoliths were characterized by their physical properties and interaction with common food fluids (i.e., water and oil).

The present research was carried out in the framework of COST Action CA18125, founded by the European Union, exploiting the expertise in cellulose porous materials of Tatiana Budtova and Marion Negrier (Mines Paris, France), and the food science and technology expertise of Francesco Ciuffarin, Stella Plazzotta, Michele Libralato, Sonia Calligaris and Lara Manzocco (University of Udine).

The obtained results open a range of possible food applications for cellulose-based porous templates.

Best regards,

Stella Plazzotta

Department of AgriFood, Environmental and Animal Sciences
University of Udine, via Sondrio 2/A, 33100 Udine, Italy
stella.plazzotta@uniud.it

Supercritical- and freeze-drying were used to prepare cellulose aerogels and cryogels

Cellulose aerogels show lower porosity and higher specific surface vs cryogels

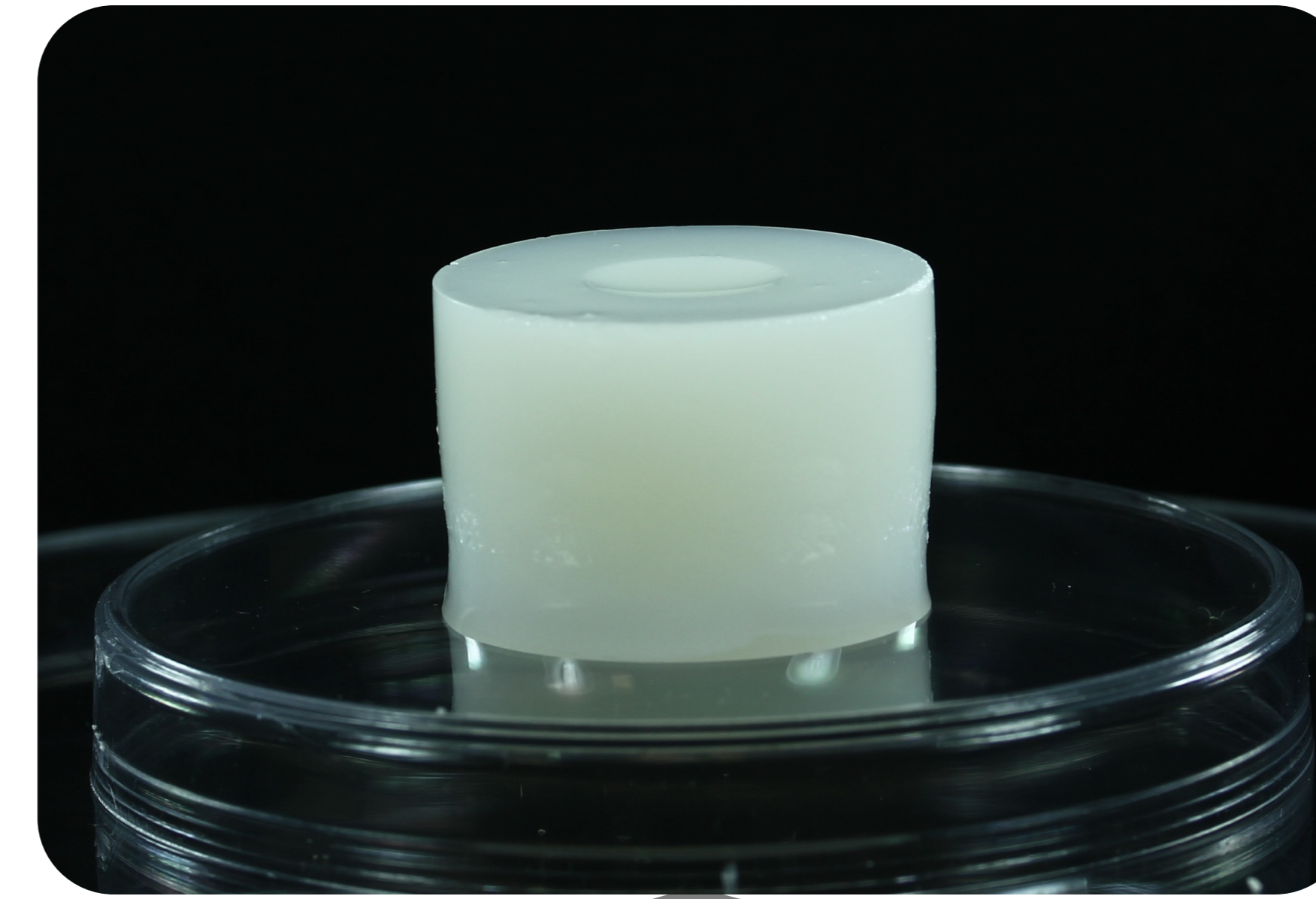
Morphology of cryogels and aerogels drives water and oil absorption kinetics

Porosity of cryogels and aerogels drives water and oil absorption at equilibrium

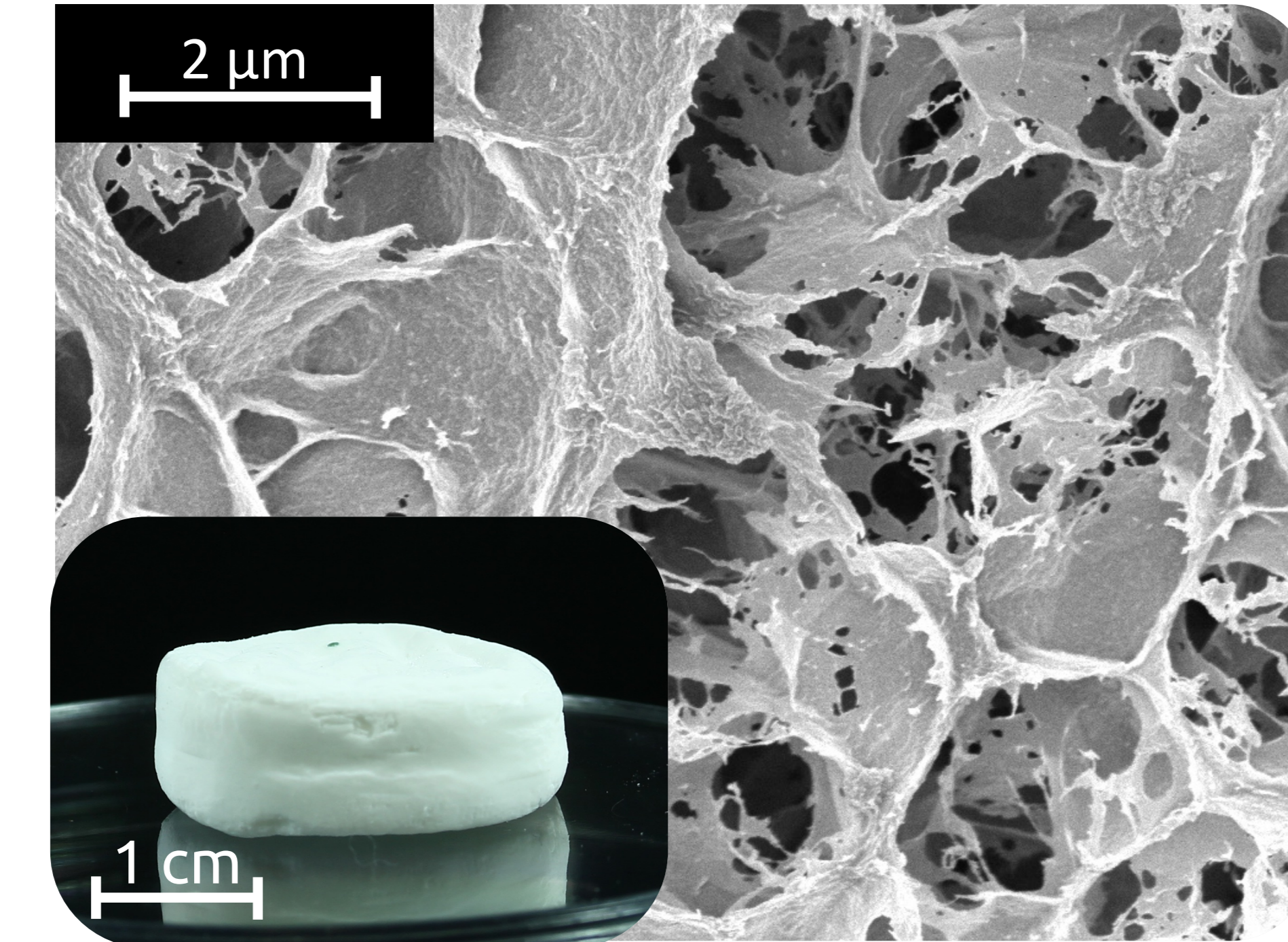
Aerogels and cryogels absorb and retain up to 8 and 12 g/g fluid, respectively

Food-grade Cellulose Hydrogel

(from solutions at 3, 4, 5%, w/w)



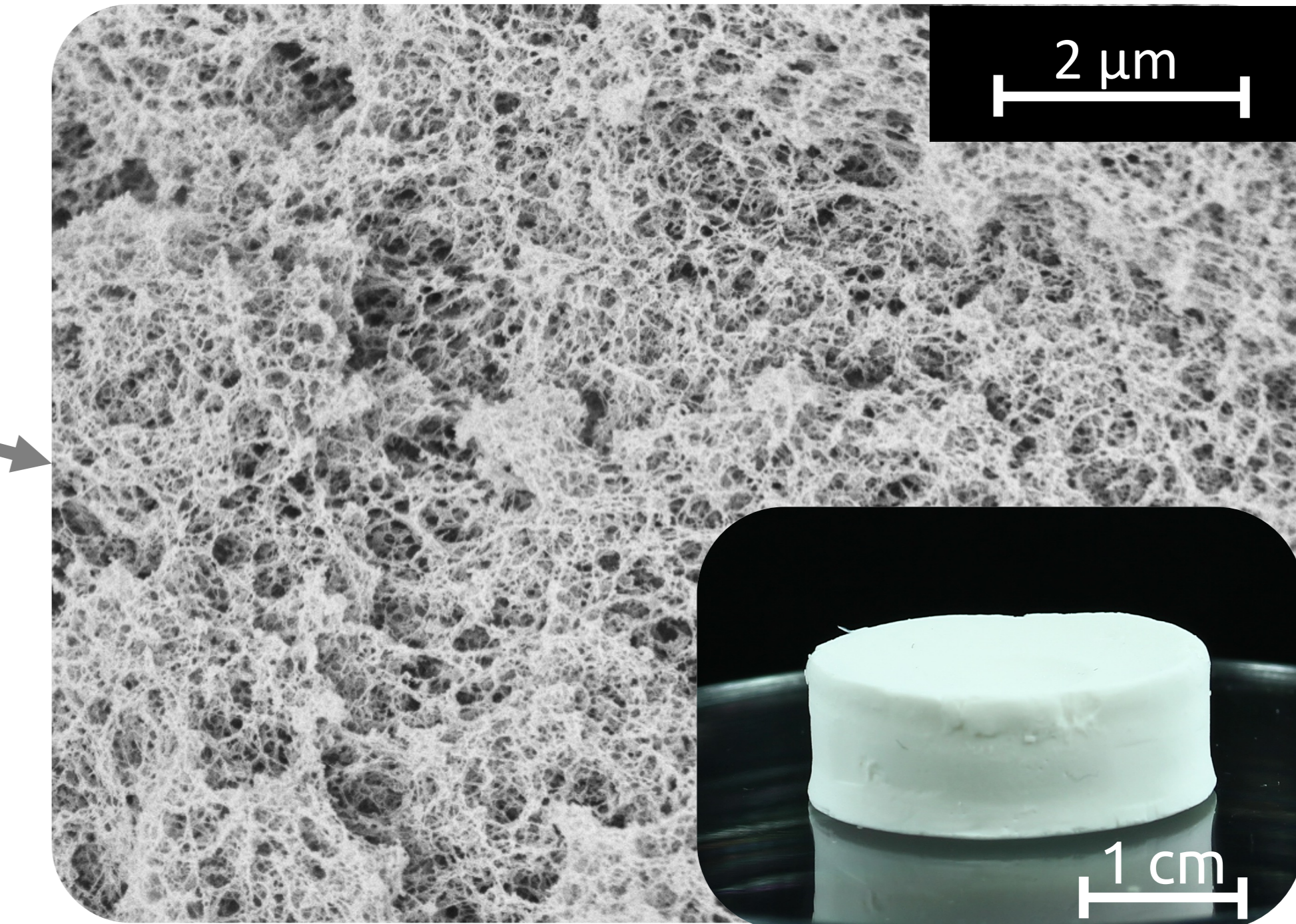
Cellulose Cryogel



Freeze Drying

Supercritical CO₂ Drying

Cellulose Aerogel



Material morphology drives oil and water absorption kinetics
Material porosity controls maximum fluid absorption

1 **Interactions of cellulose cryogels and aerogels with water and oil: structure-function**
2 **relationships**

3 **Francesco Ciuffarin¹, Marion Negrier², Stella Plazzotta^{1,*}, Michele Libralato³, Sonia**
4 **Calligaris¹, Tatiana Budtova², Lara Manzocco¹**

5 ¹ Department of Agricultural, Food, Environmental and Animal Sciences, University of Udine,
6 Via Sondrio 2/A, 33100 Udine, Italy

7 ² MINES Paris, PSL University, Center for Material Forming (CEMEF), UMR CNRS 7635,
8 CS 1027, 06904 Sophia Antipolis, France

9 ³ Polytechnic Department of Engineering and Architecture, University of Udine, Via delle
10 Scienze 206, 33100 Udine, Italy

11 *Corresponding author

12 e-mail: stella.plazzotta@uniud.it

13

14 **Abstract**

15 Food-grade porous materials, aerogels and cryogels, were prepared from cellulose hydrogels
16 obtained from solutions at increasing cellulose concentration (3, 4, 5%, w/w) by supercritical-
17 CO₂-drying (SCD) and freeze-drying (FD), respectively. The structure depended on the applied
18 drying technique, with aerogels showing a denser network with pores <200 nm in diameter, a
19 specific surface area of 370-380 m²g⁻¹, and a porosity of 92-94%. Cryogels presented larger
20 pores (2-5 μm diameter), much lower specific surface area (around 30 m²g⁻¹) and higher
21 porosity (95-96%). Structuring cellulose into aerogels and cryogels increased its capability of
22 interacting with water vapor. The absorption of water and oil was investigated as a function of
23 time and at equilibrium. While water was almost immediately absorbed by both aerogels and
24 cryogels, a much longer time was needed to reach oil absorption equilibrium. Moreover,
25 aerogels required a longer time than cryogels. Material morphology governed absorption
26 kinetics, while the absorption at equilibrium was directly dependent on material porosity rather
27 than on its morphology or material-fluid affinity. As a result, due to their lower porosity,
28 aerogels absorbed a lower amount of water or oil (4-8 g_{fluid}/g_{dry matter}) than cryogels (8-12
29 g_{fluid}/g_{dry matter}). All samples showed high fluid holding capacity (>96%); while water absorption
30 caused a firmness decrease, the firmness of oil-filled materials was the same as of the unloaded
31 ones. This study demonstrates that food-grade cellulose aerogels and cryogels can be
32 structurally designed by acting on cellulose concentration and drying technique to obtain
33 controlled food fluid loading.

34 **Keywords:** porous materials; microstructure; adsorption; absorption; loading

35

36

37 **1 Introduction**

38 Highly porous food-grade materials can be prepared by water removal from hydrogels,
39 the latter obtained thanks to the structuration ability of biopolymers (i.e., proteins and
40 polysaccharides) (García-González et al., 2019). The physical structure of the final dried
41 material strongly depends on the technology applied to remove water from the hydrogel. When
42 freeze-drying (FD) is applied, the growth of ice crystals during the freezing step induces the
43 concentration of biopolymer chains between ice crystals, eventually leading to the local
44 contraction of the gel network. As a result, the final material usually possesses large
45 macropores, low density and low internal surface area. Such materials are defined as
46 “cryostructurates” (Lozinsky, 2018; Lozinsky et al., 2003), but they are also often called
47 “cryogels”. Alternatively, supercritical-CO₂ drying (SCD) can be applied. In this case, water in
48 the hydrogel is substituted with a liquid miscible with CO₂, which, for food applications, is
49 food-grade ethanol. The resulting alcogels are then dried with supercritical CO₂. The distortions
50 in the gel network are thus theoretically minimized, and the original structure is maintained
51 (García-González et al., 2011). The obtained materials are usually characterized by high
52 porosity and a high internal surface area, mainly due to the presence of mesopores (2-50 nm).
53 Such open-pore low-density nanostructured materials are defined as aerogels.

54 The unique features of bio-based cryogels and aerogels are being explored in many
55 potential industrial fields for biomedical, environmental, cosmetic and engineering purposes
56 (García-González et al., 2019; Sharma et al., 2019; Tyshkunova et al., 2022). Recently, bio-
57 aerogels were suggested for various food applications, from delivery systems of active
58 compounds, to packaging (Manzocco, Mikkonen, et al., 2021). High potentialities of cryogels
59 and aerogels as advanced food ingredients exploitable in the modulation of food texture and
60 nutritional profile were also demonstrated. For example, cryogels and aerogels prepared from
61 κ -carrageenan, vegetable fibers, and whey proteins have been used to structure both water and
62 oil in semi-solid materials (Manzocco et al., 2017; Plazzotta et al., 2019b, 2020, 2021).
63 Hydroxypropyl methylcellulose cryogels have been proven to be effective in protecting the
64 loaded molecules (e.g., curcumin) from the harsh stomach pH, promoting their controlled
65 release, and increasing their intestinal bioaccessibility (Chuesiang et al., 2022). Similar effects
66 in the modulation of the digestion of the loaded bioactive molecules (e.g., polyunsaturated fatty
67 acids, phytosterols) have been also demonstrated for protein and starch aerogels (Plazzotta et
68 al., 2022; Selmer et al., 2019; Ubeyitogullari & Ciftci, 2019; Uchida et al., 2022).

69 Cellulose is a particularly attractive biopolymer for the preparation of food-grade cryogels
70 and aerogels. It is the most abundant polysaccharide on the Earth, not expensive, and it can also

71 be obtained from agro-industrial vegetable side streams, in a closed loop that avoids the
72 generation of large quantities of waste (Pires et al., 2022). Moreover, this non-digestible
73 carbohydrate is considered a pre-biotic, being the primary source of energy for most gut
74 microbes and acting as a gut-protection agent (Brownlee et al., 2006; David et al., 2014).
75 There are two main ways to make cellulose aerogels and cryogels: one is from nanocellulose
76 and the other is by cellulose dissolution. As nanocellulose is not in the scope of our work, only
77 aerogels and cryogels obtained *via* cellulose dissolution will be overviewed. In this technique,
78 the first step is the preparation of a cellulose solution. However, the majority of cellulose
79 solvents are far from being food-grade (Liebert, 2010). One of the very few acceptable options
80 is aqueous 7-9% NaOH. The dissolution of cellulose in NaOH-water, solution properties and
81 materials made from them have been summarized and discussed in detail (Budtova & Navard,
82 2016). The dissolution of cellulose in NaOH-water occurs at sub-zero temperatures; solutions
83 are gelling in time and gelation is faster with temperature increase (Roy et al., 2003b). To obtain
84 a hydrogel, NaOH is washed out by placing the cellulose-NaOH-water gel in successive water
85 baths. As water is cellulose antisolvent, cellulose is coagulating, keeping the shape of the
86 container in which the solution is gelled (Budtova, 2019). The obtained self-standing hydrogel
87 can be dried *via* FD or SCD, to generate cryogels (Ciolacu et al., 2016) or aerogels (Gavillon
88 & Budtova, 2008a), respectively.

89 Cellulose cryogels and aerogels, due to their unique properties, can represent innovative
90 candidates as advanced food ingredients. However, to our knowledge, the functionalities of
91 these materials in foods have not been investigated yet.

92 In this study, cryogels and aerogels were prepared by FD or SCD of cellulose hydrogels
93 obtained from cellulose-NaOH-water solutions and characterized for their structural features
94 (SEM microstructure, BET specific surface area, porosity, pore volume, and density).
95 Following, their interaction with common food fluids (i.e., water and oil) were studied, opening
96 a range of possible food applications for cellulose-based porous templates.

97
98

99 2 Materials and methods

100 2.1 Materials

101 Microcrystalline cellulose (Avicel[®], pH-101, degree of polymerization 180 as declared by the
102 manufacturer) was purchased from Sigma Aldrich. Sunflower oil was obtained from a local
103 store. Deionized water was made with System advantage A10[®], Millipore S.A.S, Molsheim,
104 France); absolute ethanol (purity > 99%) and NaOH were purchased from Fisher Chemical.
105

106 2.2 Preparation of cellulose hydrogels, cryogels, and aerogels

107 Cellulose hydrogels were prepared as follows. Microcrystalline cellulose was first dried at 50
108 °C under vacuum for at least 2 h, pre-soaked in water for a few hours and then mixed with
109 NaOH-water, pre-cooled at -16 °C, at 50 rpm using a mixer (Hei-Torque 100, Heidolph,
110 Schwabach, Germany) for 2 h in a thermostatic cooling bath (Huber Compatible Control CC1,
111 Offenburg, Germany) at -5 °C. Cellulose concentration was 3, 4, and 5 % (w/w) in 8% (w/w)
112 NaOH-water. The obtained solutions were transparent and optically homogeneous. Around 6
113 mL of solution was poured into cylindrical polypropylene vials (2.7 cm diameter) and heated
114 at 50 °C for 2 h; in these conditions, cellulose-NaOH-water solutions are gelling (Roy et al.,
115 2003a). The gels were then placed in successive water baths to dilute NaOH, as tested with pH-
116 meter (BASIC pH meter, Denver Instrument, Bohemia, USA); the resulting material was a
117 cellulose hydrogel at pH 7.0.

118 To obtain cryogels, cellulose hydrogels were frozen by immersion into liquid nitrogen (-196
119 °C) and freeze-dried for 72 h at -80 °C and 10 mTorr (Cryotec Cosmos, Saint-Gély-du-Fesc,
120 France).

121 To obtain aerogels, water in hydrogels was first replaced by ethanol, a fluid miscible with CO₂
122 (Budtova, 2019): cellulose hydrogels were placed in successive water-ethanol baths with a
123 gradual increase in ethanol concentration to completely remove water. The resulting alcogels
124 were dried with supercritical CO₂ (homemade set-up of PERSEE Mines Paris, France); the
125 details can be found elsewhere (Zou & Budtova, 2021). Briefly, alcogels were placed in a 1 L
126 autoclave, pressurized at 80 bar and 37 °C and ethanol purged. Two dynamic washing steps
127 were then performed for 1 and 2 h with a CO₂ output of 5 kg h⁻¹. In between those dynamic
128 steps, a static mode of 2 h was used, with no CO₂ output. Finally, the system was slowly
129 depressurized at 4 bar h⁻¹ and 37 °C, and cooled down to room temperature.

130 The obtained dried monoliths were stored in a desiccator containing granular silica gel at room
131 temperature until analysis.

132

133 2.3 Characterization

134 2.3.1 Image acquisition

135 Sample images were acquired using an image acquisition cabinet and a Google Pixel 6 camera
136 (Alphabet, Mountain View, California, USA). The light was provided by a LED strip properly
137 placed to minimize shadow and glare.

138

139 2.3.2 Morphology by Scanning Electron Microscopy (SEM)

140 SEM micrographs were obtained using a MAIA-3 (Tescan, Brno, Czech Republic), equipped
141 with detectors of secondary and back-scattered electrons. The internal cross-section of the
142 samples was coated with a 14 nm layer of platinum with a Quorum Q150T metallizer (Quorum
143 Technologies, East Sussex, UK) to prevent the accumulation of electrostatic charges and
144 images' defaults. The observations were performed with an acceleration voltage of 3 kV.

145

146 2.3.3 Volume variation

147 Sample volume was calculated as the volume of the cylinder whose diameter and height were
148 measured by a CD-15APXR digital caliber (Absolute AOS Digimatic, Mitutoyo Corporation,
149 Kanagawa, Japan). Volume variation (ΔV , %) during the conversion of hydrogels to cryogels
150 or aerogels was expressed as follows (eq. 1).

$$151 \quad \Delta V(\%) = \frac{V_H - V_D}{V_H} \cdot 100 \quad (\text{eq. 1})$$

152 where V_H and V_D are the volumes of the hydrogel and of the dried material (cryogel or aerogel),
153 respectively.

154

155 2.3.4 Bulk density, porosity, and pore volume

156 Bulk density (ρ_{bulk}) was measured using the Micromeritics GeoPyc 1360 Envelope Density
157 Analyzer (Norcross, Georgia, USA) with the DryFlo[®] powder as a fluid medium. Each sample
158 was measured in 5 cycles with an applied force of 27 N. Porosity (eq. 2) and pore volume (eq.
159 3) were calculated from bulk (ρ_{bulk}) and cellulose skeletal density ($\rho_{skeletal} = 1.5 \text{ g cm}^{-3}$, Sun,
160 2005):

$$161 \quad \text{Porosity} (\%) = \left(1 - \frac{\rho_{bulk}}{\rho_{skeletal}}\right) \cdot 100 \quad (\text{eq. 2})$$

162

$$163 \quad \text{Pore volume} (\text{cm}^3 \text{g}^{-1}) = \frac{1}{\rho_{bulk}} - \frac{1}{\rho_{skeletal}} \quad (\text{eq. 3})$$

164

165 **2.3.5 Specific surface area**

166 The specific surface area was determined by measuring N₂-adsorption isotherm at 77 K with
167 the Micromeritics ASAP 2020 (Norcross, Georgia, USA) and using Brunauer, Emmett and
168 Teller (BET) approach (Brunauer et al., 1938). Prior to measurements, samples were degassed
169 5 h at 70 °C.

170

171 **2.3.6 Firmness**

172 Firmness was measured by a uniaxial compression test using an Instron 4301 (Instron LTD.,
173 High Wycombe, UK). Samples were tested at ambient conditions using a 6.2 mm diameter
174 cylindrical probe mounted on a 1000 N compression head at a 25 mm/min crosshead speed.
175 Force-distance curves were obtained from the compression tests and firmness was taken as the
176 maximum force (N) required to penetrate the sample for 2 mm.

177

178 **2.3.7 Water vapor adsorption**

179 The water vapor sorption isotherms were recorded with the ProUmid "Vsorp Basic" dynamic
180 vapor sorption analyzer system (ProUmid, Ulm, Germany). The monoliths were cut using a
181 microtome blade to obtain 0.4 g samples. The latter were placed in aluminium plates (86 mm
182 in diameter) and kept in a climatic chamber at 25 ± 0.1 °C. The percentage of relative humidity
183 (RH) in the sample headspace was automatically increased from 0 ± 0.1% RH to 90 ± 0.1% RH
184 with 10% RH steps. The equilibrium of each step was considered to be reached when sample
185 mass variation was lower than 0.01% for at least 300 min. The water vapor isotherms were
186 expressed as moisture (g_{H₂O}/g_{dry matter}) as a function of sample water activity (a_w), which
187 corresponds to RH/100 in the headspace of the sample at equilibrium conditions.

188

189 **2.3.8 Water and oil absorption kinetics**

190 Cryogels and aerogels were manually cut into cubes of 1 cm³ volume and weighted (W₀). Cubes
191 were immersed into Petri plates containing water or sunflower oil at room temperature (22 °C).
192 At defined time intervals, samples were withdrawn, wiped with absorbent paper, and weighed
193 (W_t). The experiment was carried out until a constant weight was reached (*plateau* or
194 equilibrium value), as indicated by no weight variation in 3 consecutive measures. Absorbed
195 water or oil at each time was expressed as the ratio between weight gain at time t (min) and the
196 initial weight of the cryogel or aerogel sample (eq. 4).

$$197 \quad \text{Absorbed solvent (g}_{fluid}/\text{g}_{dry matter}) = \frac{(W_t - W_0)}{W_0} \quad (\text{eq. 4})$$

198 The maximum solvent absorption capacity was taken at equilibrium.

199

200 **2.3.9 Water and oil holding capacity**

201 When the absorption reached the equilibrium, around 100-200 mg of sample (W_1) was placed
202 into 1.5 mL microtubes and centrifuged at 15,000g for 30 min using a microcentrifuge (Mikro
203 120, Hettich Zentrifugen, Andreas Hettich GmbH and Co, Tuttlingen, Germany). After
204 centrifugation, the released fluid was accurately wiped using absorbing paper and the sample
205 was weighted again (W_2). Water (WHC) and oil holding capacity (OHC) were calculated as the
206 percentage ratio between the weight of fluid retained in the sample after centrifugation and the
207 total fluid weight initially present (eq. 5).

$$208 \quad \text{Fluid Holding Capacity (\%)} = \frac{S \cdot W_1 - (W_1 - W_2)}{S \cdot W_1} \cdot 100 \quad (\text{eq. 5})$$

209 where S represents the weight fraction (%) of the fluid initially present in the sample.

210

211 **2.3.10 Data analysis**

212 Data were expressed as the mean \pm standard error of at least two measurements from two
213 experimental replicates ($n \geq 4$). Statistical analysis was performed by using R v. 4.0.3 (The R
214 Foundation for Statistical Computing). ANOVA test was used to determine statistically
215 significant differences between means ($p < 0.05$). Bartlett's test was used to check the
216 homogeneity of variance ($p \geq 0.05$) and the Tukey test was used as *post-hoc* test ($p < 0.05$).

217

218

219

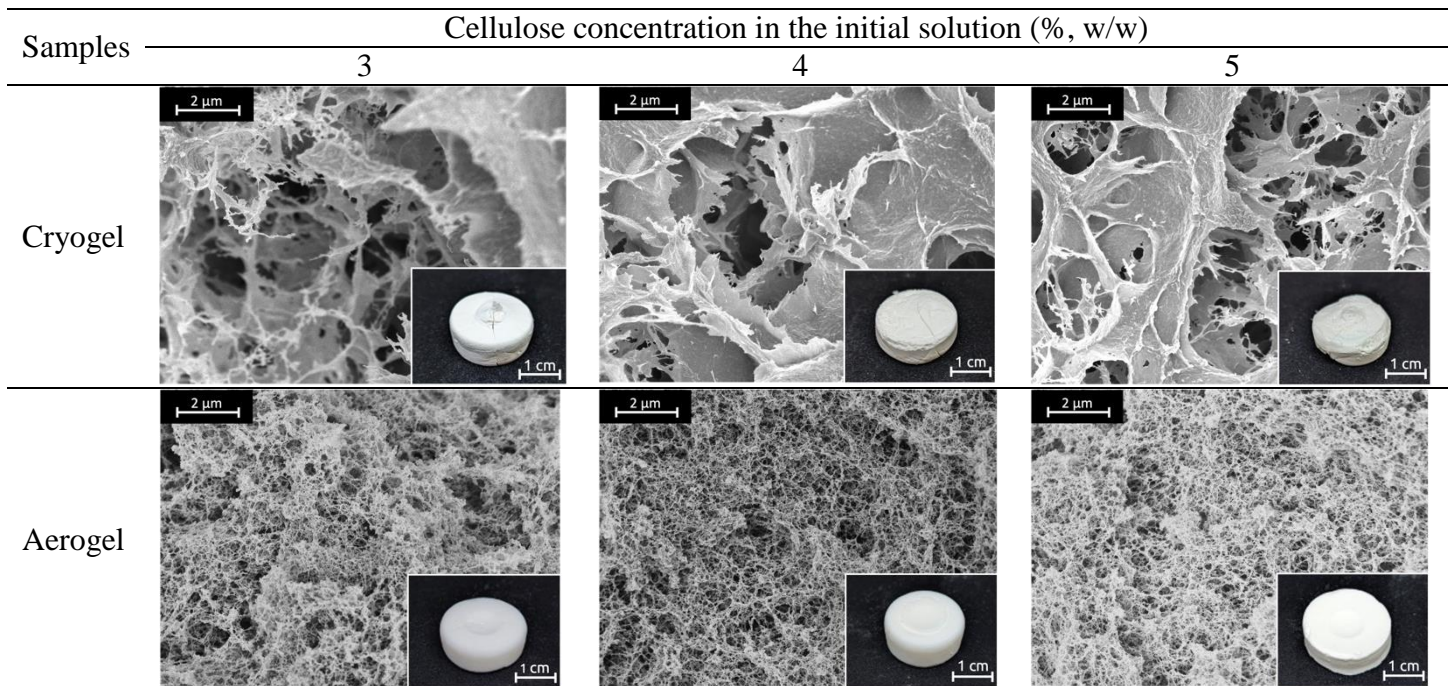
220 **3 Results and discussion**

221 **3.1 Characterization of cryogels and aerogels**

222 Table 1 shows the visual appearance and microstructure of cryogels and aerogels prepared *via*
223 freeze-drying (FD) and supercritical-CO₂ drying (SCD), respectively, of hydrogels obtained
224 from cellulose solutions containing 3, 4, 5% (w/w) cellulose.

225

226 Table 1. Visual appearance and SEM microstructure of cryogels and aerogels prepared from
227 cellulose solutions containing 3, 4, 5% (w/w) cellulose.



228

229 Both cryogels and aerogels appeared visually opaque (Buchtová & Budtova, 2016; Gavillon &
230 Budtova, 2008b). Cryogels showed an uneven surface with evident cracking, whereas aerogels
231 appeared more homogeneous without visible cracks (insets in Table 1). SEM revealed
232 significant differences between aerogel and cryogel morphology (Table 1). In cryogels, larger
233 pores (around and below 2-5 μm) with flat walls were observed, in agreement with previous
234 literature (Buchtová & Budtova, 2016). Although ice crystals sublimation during FD avoids
235 liquid-vapor interfaces and thus capillary surface tension (Fricke & Tillotson, 1997), ice crystal
236 formation and growth during hydrogel freezing force cellulose chains to locally collapse and
237 concentrate, resulting in large pores and non-porous pore walls (Assegehegn et al., 2019). By
238 contrast, aerogels showed a more homogeneous microstructure (Table 1), characterized by a
239 fibrillated network, with the majority of pores of diameter lower than 200 nm.

240 The conversion of hydrogels into cryogels led to a slight volume increase, as indicated by the
241 positive volume variation (Table 1). This result can be attributed to the ice crystal growth during

242 FD (Assegehegn et al., 2019). By contrast, aerogel preparation caused volume contraction
 243 (Table 1), which can be attributed to the increased difference in solubility parameters between
 244 cellulose (39 MPa^{0.5}), ethanol (26.5 MPa^{0.5}) and CO₂ (around 5 - 8 MPa^{0.5} for the supercritical
 245 CO₂ in the conditions used in the present study) (Hansen, 2007; Zhang et al., 2017) As a
 246 consequence, cryogels presented lower density than the aerogels made from cellulose solutions
 247 of the same concentration (Table 2). As expected, higher cellulose concentrations in the initial
 248 solution led to both cryogels and aerogels of higher density. The porosity of both materials was
 249 higher than 90% and it was slightly lower for aerogels as compared to cryogels. The pore
 250 volume of cryogels was higher than that of aerogels, and for both types of materials pore volume
 251 decreased with density increase (Table 2).

252

253 Table 2. Volume variation, bulk density, porosity, pore volume, BET-specific surface area, and
 254 firmness of cryogels and aerogels prepared from cellulose solutions containing 3, 4, 5% (w/w)
 255 cellulose.

Sample	Cellulose solution concentration (%)	ΔV (%)	Bulk density (g cm ⁻³)	Porosity (%)	Pore Volume (cm ³ g ⁻¹)	BET (m ² g ⁻¹)	Firmness (N)
Cryogel	3	9.5 ± 4.7 ^b	0.056 ± 0.002 ^d	96.2 ± 0.1 ^a	17.01 ± 0.60 ^a	28 ± 0 ^b	10.44 ± 1.1 ^e
	4	7.7 ± 1.8 ^b	0.071 ± 0.002 ^c	95.3 ± 0.1 ^b	13.40 ± 0.37 ^b	31 ± 2 ^b	19.9 ± 0.57 ^d
	5	4.9 ± 0.8 ^c	0.077 ± 0.004 ^b	94.9 ± 0.3 ^b	12.30 ± 0.64 ^b	30 ± 1 ^b	25.1 ± 0.48 ^c
Aerogel	3	- 25.9 ± 2.4 ^a	0.077 ± 0.007 ^b	93.8 ± 0.3 ^c	10.08 ± 0.57 ^c	384 ± 4 ^a	21.0 ± 0.36 ^d
	4	- 23.3 ± 3.2 ^a	0.098 ± 0.005 ^{ab}	93.5 ± 0.4 ^{cd}	9.54 ± 0.59 ^c	380 ± 10 ^a	35.8 ± 1.57 ^b
	5	- 20.8 ± 2.6 ^a	0.112 ± 0.006 ^a	92.9 ± 0.2 ^d	8.69 ± 0.21 ^c	371 ± 11 ^a	44.1 ± 1.08 ^a

256 ^{a-c}: In the same column, mean values indicated by different letters are statistically different (p
 257 < 0.05).

258

259 Specific surface area (BET), which reflects the presence of mesopores and small macropores
 260 (< 200 nm), was more than 10-times higher for aerogels as compared to cryogels (Table 2), in
 261 line with SEM observations (Table 1) and results reported in the literature for bio-aerogels
 262 (Buchtová & Budtova, 2016; Zou & Budtova, 2021). It should be noted that large macropores
 263 are not detected by BET approach, and thus a complete pore size distribution is not possible
 264 based on BET results solely (Robitzer et al., 2011; Zou & Budtova, 2021).

265 As a result of the lower density, cryogels presented lower firmness as compared to that of the
 266 aerogels prepared from cellulose solutions of the same concentration (Table 2). This is in line
 267 with literature results. For instance, κ -carrageenan cryogels and aerogels showed firmness
 268 values of 1.2 and 47.1 N, respectively (Plazzotta et al., 2019a); similarly, cryogels and aerogels
 269 prepared from whey protein hydrogels showed firmness of 18.5 and 29.5 N, respectively
 270 (Manzocco et al., 2021). As expected, since density increased with cellulose concentration, the
 271 firmness followed a similar trend, similarly to the previously reported trend for the Young's
 272 modulus of various porous cellulose materials (Buchtová et al., 2019; Schestakow et al., 2016).

273 3.2 Interaction with water and oil

274 In order to analyze the capacity of cellulose cryogels and aerogels to interact with water vapor,
275 moisture adsorption isotherms were assessed. As a representative example, Figure 1 shows data
276 relevant to cryogels and aerogels made from 5% (w/w) cellulose solutions (density $0.077 \pm$
277 0.004 and $0.112 \pm 0.006 \text{ g cm}^{-3}$, respectively). The adsorption isotherm of microcrystalline
278 cellulose is shown for comparison.

279 Microcrystalline cellulose isotherm was consistent with literature data (Portugal et al., 2010).
280 A steady increase in the moisture content was observed in the a_w region up to 0.7, related to the
281 saturation of hydrophilic sites on the cellulose surface. Upon further a_w increase ($a_w > 0.7$), an
282 inflexion point in the adsorption isotherm was observed, followed by higher moisture
283 adsorption (Figure 1). This is attributed to the cleavage of cellulose intermolecular hydrogen
284 bonds by water, which interacts with cellulose and promotes fiber swelling (Portugal et al.,
285 2010). The transformation of microcrystalline cellulose into cryogels and aerogels did not
286 change the form of the isotherm but resulted in a shift towards higher moisture values over the
287 entire a_w range (Figure 1), indicating an increased ability of cellulose to interact with water
288 vapor. Water vapor adsorption isotherms were also assessed for cryogels and aerogels prepared
289 from 3 and 4% (w/w) cellulose solution. Data shown in Appendix Figure A.1 indicate no effect
290 of cellulose concentration in the solution on the moisture uptake of both cryogels and aerogels.
291 It is known that microcrystalline cellulose actually contains a rather high crystalline fraction,
292 limiting the interactions with water vapor (Bhandari, 2013). The conversion of microcrystalline
293 cellulose into cellulose II-based cryogels and aerogels decreases the crystalline fraction, thus
294 increasing cellulose accessibility to water vapor (Yue et al., 2012).

295 Figure 1 also shows that the isotherms were negligibly affected by the drying technique (freeze-
296 drying vs supercritical drying), and not influenced by material porosity or specific surface area
297 either (Table 2).

298 The possibility of using cellulose cryogels and aerogels as innovative food ingredients requires
299 the knowledge of their ability to absorb and retain the most common liquids used in foods,
300 namely water and oil. The kinetics of water and oil absorption by aerogels and cryogels is
301 shown in Figure 2. Upon contact with water, an extremely fast absorption was observed for all
302 the samples (Figure 2), so that the absorption equilibrium was reached after a few seconds. The
303 absorption of oil was from one to three orders of magnitude slower than that of water (Figure
304 2). The faster absorption of water as compared to oil by both cryogels and aerogels can be
305 attributed to the hydrophilic nature of cellulose as well as to the lower viscosity of water (0.001
306 Pa s at $25 \text{ }^\circ\text{C}$) as compared to that of sunflower oil (0.060 Pa s at $25 \text{ }^\circ\text{C}$) (Lucas-Washburn
307 equation).

308 Cryogels were previously found to absorb fluids faster than aerogels. For example, in the case
309 of cryogels, oil absorption approached the equilibrium within 15-60 min depending on material
310 porosity. Instead, aerogels showed a more gradual oil absorption, which levelled off only after
311 200-250 min. These differences in fluid absorption kinetics can be attributed to the different
312 morphology of cryogels and aerogels. In particular, aerogels present much smaller pores as
313 compared to cryogels, as seen in Table 1 and also deduced from the specific surface area of the
314 materials (Table 2).

315 The maximum water and oil absorption values (or equilibrium values in Figure 2) of all the
316 prepared materials were plotted as a function of porosity (Figure 3). These values varied from
317 4 to 8 $\text{g}_{\text{fluid}}/\text{g}_{\text{dry matter}}$ for aerogels and from 8 to 13 $\text{g}_{\text{fluid}}/\text{g}_{\text{dry matter}}$ for cryogels, due to different
318 material porosity (see Table 2). Interestingly, all equilibrium values fell on the same linear trend
319 ($p \geq 0.05$) as a function of material porosity despite the hydrophilic nature of cellulose, and not
320 depending on the type of liquid (oil vs water) or pore dimensions. This highlights the pivotal
321 role of material porosity on fluid uptake values at equilibrium.

322 Literature reports using porous cellulose for the absorption of various liquids. Most studies used
323 functionalized freeze-dried cellulose II for oil absorption. After silylation (Lin et al., 2015),
324 chemical vapor deposition (Liao et al., 2016) or plasma treatment (Zhang et al., 2016),
325 absorption values were in the range from 20 to 60 $\text{g}_{\text{oil}}/\text{g}_{\text{dry matter}}$. Similar values were also
326 reported for functionalized freeze-dried nanocellulose. By contrast, very few examples are
327 known about the absorption behavior of neat cellulose II aerogels. In the study of Chin et al.
328 (2014) cellulose coated with TiO_2 showed a five times higher oil absorption capacity (up to 28
329 $\text{g}_{\text{oil}}/\text{g}_{\text{dry matter}}$), as compared to its non-coated counterpart (5 $\text{g}_{\text{oil}}/\text{g}_{\text{dry matter}}$). The results acquired
330 in this study (Figures 2 and 3) demonstrate that cellulose aerogels and cryogels absorb large
331 quantities of water and oil without any chemical modification. This is particularly relevant for
332 the food application of these porous materials: in fact, despite resulting in high fluid absorption,
333 the chemical modifications cited above are not acceptable for food applications.

334 The effect of water and oil absorption on cryogel and aerogel firmness is reported in Figure 4,
335 where firmness values of cryogels and aerogels prior to and after water and oil absorption are
336 plotted against porosity. Water absorption caused a significant decrease in sample firmness as
337 compared to the dried materials (Figure 4). Differently from water-absorbed samples, oil
338 absorption had a negligible effect on cryogel and aerogel firmness (Figure 4). The different
339 effect of water and oil absorption on cryogels and aerogels firmness is probably attributable to
340 the high hygroscopicity of cellulose, which causes the hydration of the cellulose network,
341 weakening it, as also demonstrated for other porous materials based on vegetable fibers and

342 proteins. By contrast, oil would simply fill the voids without significantly interacting with the
343 polymer network (Manzocco, Plazzotta, et al., 2021; Plazzotta et al., 2018).
344 Finally, the ability of cryogels and aerogels to retain the absorbed liquid was evaluated under
345 centrifugal stress. All the samples showed similar ($p \geq 0.05$) high water and oil holding capacity,
346 with values higher than 96%, independently on drying technique, material porosity and specific
347 surface area. These results were expected for aerogels, due to the ability of small pores (Table
348 1) to strongly entrap the fluid. Similar oil holding capacity (OHC) values (96.3 and 83.4%),
349 were obtained for whey protein and κ -carrageenan aerogels, which presented pore sizes around
350 100 and 400 nm, respectively (Manzocco et al., 2017; Manzocco, Plazzotta, et al., 2021;
351 Plazzotta et al., 2019a). Remarkably, cellulose cryogels showed much higher water and oil
352 holding capacity values than those reported in the literature. For example, cryogels prepared
353 from both whey proteins and κ -carrageenan showed an OHC lower than 50% (Plazzotta et al.,
354 2019b, 2020). This result was attributed to the lower capillary forces in the cryogel network,
355 because of very large pores (up to 900 μm) (Manzocco, Plazzotta, et al., 2021; Plazzotta et al.,
356 2019a). One of the reasons of the high water and oil holding capacity of the cellulose cryogels
357 is rather small pore size, around 2-5 μm (Table 1), resulting in capillary forces that are much
358 higher than in bio-based cryogels cited above.

359

360 **Conclusions**

361 Cellulose aerogels and cryogels were made via supercritical- and freeze-drying, respectively,
362 and tested for the absorption and holding capacity of water and vegetal oil. All materials
363 possessed very high porosity, above 90%. By varying drying techniques, materials with
364 different morphology were obtained: aerogels had a fine ramified network with pore size below
365 200 nm, while cryogels presented pores of few microns and lower, and continuous flat pore
366 walls.

367 The kinetics of water and oil absorption was investigated: water was absorbed by aerogels and
368 cryogels within one minute, while oil absorption was much slower due to oil higher viscosity
369 and hydrophobicity. Oil absorption by cryogels was much faster than by aerogels, 15-60 min
370 vs 200-250 min, respectively. This phenomenon was attributed to material morphology as
371 described above.

372 The maximum absorption of oil and of water was proportional to material porosity, and all
373 experimental values fell on the same linear plot. Porosity turned out to be the main parameter
374 governing fluid absorption at equilibrium, which did not depend on material morphology or
375 fluid polarity.

376 Finally, the water and oil holding capacity and firmness of aerogels and cryogels, both before
377 and after water and oil loading, were analyzed. Firmness decreased with material porosity
378 increase, as expected. Water loading caused firmness decrease as compared to the unloaded
379 aerogels and cryogels, while the firmness of materials filled with oil was comparable to the one
380 with air in the pores.

381 These interesting results open new prospects in using cellulose aerogels and cryogels in food
382 applications. Indeed, cellulose-based materials entrapping high amounts of water or oil can find
383 wide applications in the food sector. On one side, their functionalities can be used to develop
384 tailored ingredients, able to modulate food textural, sensory, and nutritional properties. On the
385 other hand, they could represent tunable templates for structuring novel foods, including animal
386 food analogues.

387

388 **Funding**

389 Work was carried out in the framework of COST Action CA18125 “Advanced Engineering and
390 Research of aeroGels for Environment and Life Sciences” (AERoGELS), funded by the
391 European Commission.

392

393 **Declaration of Competing Interest**

394 The authors declare that they have no known competing financial interests or personal
395 relationships that could have appeared to influence the work reported in this paper.

396

397 **References**

- 398 Assegehegn, G., Brito-de la Fuente, E., Franco, J. M., & Gallegos, C. (2019). The Importance
399 of Understanding the Freezing Step and Its Impact on Freeze-Drying Process
400 Performance. In *Journal of Pharmaceutical Sciences* (Vol. 108, Issue 4).
401 <https://doi.org/10.1016/j.xphs.2018.11.039>
- 402 Bhandari, B. (2013). 1 - Introduction to food powders BT - Handbook of Food Powders.
403 *Woodhead Publishing Series in Food Science, Technology and Nutrition*.
- 404 Brownlee, I., Dettmar, P., Strugala, V., & Pearson, J. (2006). The Interaction of Dietary
405 Fibres with the Colon. *Current Nutrition & Food Science*, 2(3).
406 <https://doi.org/10.2174/157340106778017896>
- 407 Brunauer, S., Emmett, P. H., & Teller, E. (1938). Adsorption of Gases in Multimolecular
408 Layers. *Journal of the American Chemical Society*, 60(2).
409 <https://doi.org/10.1021/ja01269a023>
- 410 Buchtová, N., & Budtova, T. (2016). Cellulose aero-, cryo- and xerogels: towards
411 understanding of morphology control. *Cellulose*, 23(4), 2585–2595.
412 <https://doi.org/10.1007/s10570-016-0960-8>
- 413 Buchtová, N., Pradille, C., Bouvard, J.-L., & Budtova, T. (2019). Mechanical properties of
414 cellulose aerogels and cryogels. *Soft Matter*, 15(39), 7901–7908.
415 <https://doi.org/10.1039/C9SM01028A>
- 416 Budtova, T. (2019). Cellulose II aerogels: a review. In *Cellulose* (Vol. 26, Issue 1, pp. 81–
417 121). <https://doi.org/10.1007/s10570-018-2189-1>
- 418 Budtova, T., & Navard, P. (2016). Cellulose in NaOH–water based solvents: a review. In
419 *Cellulose* (Vol. 23, Issue 1). <https://doi.org/10.1007/s10570-015-0779-8>
- 420 Chuesiang, P., Zhang, J., Choi, E., Yoon, I. S., Kim, J. T., & Shin, G. H. (2022). Observation
421 of curcumin-loaded hydroxypropyl methylcellulose (HPMC) oleogels under in vitro lipid
422 digestion and in situ intestinal absorption in rats. *International Journal of Biological*
423 *Macromolecules*, 208. <https://doi.org/10.1016/j.ijbiomac.2022.03.120>
- 424 Ciolacu, D., Rudaz, C., Vasilescu, M., & Budtova, T. (2016). Physically and chemically
425 cross-linked cellulose cryogels: Structure, properties and application for controlled
426 release. *Carbohydrate Polymers*, 151, 392–400.
427 <https://doi.org/10.1016/j.carbpol.2016.05.084>
- 428 David, L. A., Maurice, C. F., Carmody, R. N., Gootenberg, D. B., Button, J. E., Wolfe, B. E.,
429 Ling, A. v., Devlin, A. S., Varma, Y., Fischbach, M. A., Biddinger, S. B., Dutton, R. J.,
430 & Turnbaugh, P. J. (2014). Diet rapidly and reproducibly alters the human gut
431 microbiome. *Nature*, 505(7484). <https://doi.org/10.1038/nature12820>
- 432 Fricke, J. U., & Tillotson, T. (1997). Aerogels: production, characterization, and applications.
433 *Thin Solid Films*, 297(1–2), 212–223. [https://doi.org/10.1016/S0040-6090\(96\)09441-2](https://doi.org/10.1016/S0040-6090(96)09441-2)
- 434 García-González, C. A., Alnaief, M., & Smirnova, I. (2011). Polysaccharide-based aerogels -
435 Promising biodegradable carriers for drug delivery systems. In *Carbohydrate Polymers*
436 (Vol. 86, Issue 4). <https://doi.org/10.1016/j.carbpol.2011.06.066>
- 437 García-González, C. A., Budtova, T., Durães, L., Erkey, C., del Gaudio, P., Gurikov, P.,
438 Koebel, M., Liebner, F., Neagu, M., & Smirnova, I. (2019). An opinion paper on
439 aerogels for biomedical and environmental applications. In *Molecules* (Vol. 24, Issue 9).
440 <https://doi.org/10.3390/molecules24091815>
- 441 Gavillon, R., & Budtova, T. (2008a). Aerocellulose: New Highly Porous Cellulose Prepared
442 from Cellulose–NaOH Aqueous Solutions. *Biomacromolecules*, 9(1), 269–277.
443 <https://doi.org/10.1021/bm700972k>
- 444 Gavillon, R., & Budtova, T. (2008b). Aerocellulose: New Highly Porous Cellulose Prepared
445 from Cellulose–NaOH Aqueous Solutions. *Biomacromolecules*, 9(1), 269–277.
446 <https://doi.org/10.1021/bm700972k>

- 447 Hansen, C. M. (2007). *Hansen Solubility Parameters*. CRC Press.
 448 <https://doi.org/10.1201/9781420006834>
- 449 Liebert, T. (2010). *Cellulose Solvents – Remarkable History, Bright Future* (pp. 3–54).
 450 <https://doi.org/10.1021/bk-2010-1033.ch001>
- 451 Lozinsky, V. (2018). Cryostructuring of Polymeric Systems. 50.† Cryogels and Cryotropic
 452 Gel-Formation: Terms and Definitions. *Gels*, 4(3), 77.
 453 <https://doi.org/10.3390/gels4030077>
- 454 Lozinsky, V., Galaev, I. Yu., Plieva, F. M., Savina, I. N., Jungvid, H., & Mattiasson, B.
 455 (2003). Polymeric cryogels as promising materials of biotechnological interest. *Trends in*
 456 *Biotechnology*, 21(10), 445–451. <https://doi.org/10.1016/j.tibtech.2003.08.002>
- 457 Manzocco, L., Mikkonen, K. S., & García-González, C. A. (2021). Aerogels as porous
 458 structures for food applications: Smart ingredients and novel packaging materials. In
 459 *Food Structure* (Vol. 28). <https://doi.org/10.1016/j.foostr.2021.100188>
- 460 Manzocco, L., Plazzotta, S., Powell, J., de Vries, A., Rousseau, D., & Calligaris, S. (2021).
 461 Structural characterisation and sorption capability of whey protein aerogels obtained by
 462 freeze-drying or supercritical drying. *Food Hydrocolloids*, 122.
 463 <https://doi.org/10.1016/j.foodhyd.2021.107117>
- 464 Manzocco, L., Valoppi, F., Calligaris, S., Andreatta, F., Spilimbergo, S., & Nicoli, M. C.
 465 (2017). Exploitation of κ -carrageenan aerogels as template for edible oleogel
 466 preparation. *Food Hydrocolloids*, 71, 68–75.
 467 <https://doi.org/10.1016/j.foodhyd.2017.04.021>
- 468 Pires, J. R. A., Souza, V. G. L., Gomes, L. A., Coelho, I. M., Godinho, M. H., & Fernando,
 469 A. L. (2022). Micro and nanocellulose extracted from energy crops as reinforcement
 470 agents in chitosan films. *Industrial Crops and Products*, 186, 115247.
 471 <https://doi.org/10.1016/j.indcrop.2022.115247>
- 472 Plazzotta, S., Alongi, M., de Berardinis, L., Melchior, S., Calligaris, S., & Manzocco, L.
 473 (2022). Steering protein and lipid digestibility by oleogelation with protein aerogels.
 474 *Food & Function*. <https://doi.org/10.1039/D2FO01257J>
- 475 Plazzotta, S., Calligaris, S., & Manzocco, L. (2018). Innovative bioaerogel-like materials
 476 from fresh-cut salad waste via supercritical-CO₂-drying. *Innovative Food Science and*
 477 *Emerging Technologies*, 47. <https://doi.org/10.1016/j.ifset.2018.04.022>
- 478 Plazzotta, S., Calligaris, S., & Manzocco, L. (2019a). Structure of oleogels from κ -
 479 carrageenan templates as affected by supercritical-CO₂-drying, freeze-drying and
 480 lettuce-filler addition. *Food Hydrocolloids*, 96, 1–10.
 481 <https://doi.org/10.1016/j.foodhyd.2019.05.008>
- 482 Plazzotta, S., Calligaris, S., & Manzocco, L. (2019b). Structure of oleogels from κ -
 483 carrageenan templates as affected by supercritical-CO₂-drying, freeze-drying and
 484 lettuce-filler addition. *Food Hydrocolloids*, 96, 1–10.
 485 <https://doi.org/10.1016/j.foodhyd.2019.05.008>
- 486 Plazzotta, S., Calligaris, S., & Manzocco, L. (2020). Structural characterization of oleogels
 487 from whey protein aerogel particles. *Food Research International*, 132, 109099.
 488 <https://doi.org/10.1016/j.foodres.2020.109099>
- 489 Plazzotta, S., Jung, I., Schroeter, B., Subrahmanyam, R. P., Smirnova, I., Calligaris, S.,
 490 Gurikov, P., & Manzocco, L. (2021). Conversion of whey protein aerogel particles into
 491 oleogels: Effect of oil type on structural features. *Polymers*, 13(23).
 492 <https://doi.org/10.3390/polym13234063>
- 493 Portugal, I., Dias, V. M., Duarte, R. F., & Evtuguin, D. v. (2010). Hydration of cellulosesilica
 494 hybrids assessed by sorption isotherms. *Journal of Physical Chemistry B*, 114(11).
 495 <https://doi.org/10.1021/jp911270y>
- 496 Robitzer, M., Renzo, F. di, & Quignard, F. (2011). Natural materials with high surface area.
 497 Physisorption methods for the characterization of the texture and surface of

498 polysaccharide aerogels. *Microporous and Mesoporous Materials*, 140(1–3), 9–16.
 499 <https://doi.org/10.1016/j.micromeso.2010.10.006>

500 Roy, C., Budtova, T., & Navard, P. (2003a). Rheological properties and gelation of aqueous
 501 cellulose - NaOH solutions. *Biomacromolecules*, 4(2).
 502 <https://doi.org/10.1021/bm020100s>

503 Roy, C., Budtova, T., & Navard, P. (2003b). Rheological Properties and Gelation of Aqueous
 504 Cellulose–NaOH Solutions. *Biomacromolecules*, 4(2), 259–264.
 505 <https://doi.org/10.1021/bm020100s>

506 Schestakow, M., Karadagli, I., & Ratke, L. (2016). Cellulose aerogels prepared from an
 507 aqueous zinc chloride salt hydrate melt. *Carbohydrate Polymers*, 137.
 508 <https://doi.org/10.1016/j.carbpol.2015.10.097>

509 Selmer, I., Karnetzke, J., Kleemann, C., Lehtonen, M., Mikkonen, K. S., Kulozik, U., &
 510 Smirnova, I. (2019). Encapsulation of fish oil in protein aerogel micro-particles. *Journal*
 511 *of Food Engineering*, 260, 1–11. <https://doi.org/10.1016/j.jfoodeng.2019.04.016>

512 Sun, C. (2005). True density of microcrystalline cellulose. *Journal of Pharmaceutical*
 513 *Sciences*, 94(10). <https://doi.org/10.1002/jps.20459>

514 Tyshkunova, I. v., Poshina, D. N., & Skorik, Y. A. (2022). Cellulose Cryogels as Promising
 515 Materials for Biomedical Applications. In *International Journal of Molecular Sciences*
 516 (Vol. 23, Issue 4). <https://doi.org/10.3390/ijms23042037>

517 Ubeyitogullari, A., & Ciftci, O. N. (2019). In vitro bioaccessibility of novel low-crystallinity
 518 phytosterol nanoparticles in non-fat and regular-fat foods. *Food Research International*,
 519 123, 27–35. <https://doi.org/10.1016/j.foodres.2019.04.014>

520 Uchida, J., Takahashi, Y., Katsurao, T., & Sakabe, H. (2022). One-step solvent-free synthesis
 521 of carbon dot-based layered composites exhibiting color-tunable photoluminescence.
 522 *RSC Advances*, 12(14). <https://doi.org/10.1039/d2ra00312k>

523 Yue, Y., Zhou, C., French, A. D., Xia, G., Han, G., Wang, Q., & Wu, Q. (2012). Comparative
 524 properties of cellulose nano-crystals from native and mercerized cotton fibers. *Cellulose*,
 525 19(4). <https://doi.org/10.1007/s10570-012-9714-4>

526 Zhang, M., Dou, M., Wang, M., & Yu, Y. (2017). Study on the solubility parameter of
 527 supercritical carbon dioxide system by molecular dynamics simulation. *Journal of*
 528 *Molecular Liquids*, 248, 322–329. <https://doi.org/10.1016/j.molliq.2017.10.056>

529 Zou, F., & Budtova, T. (2021). Tailoring the morphology and properties of starch aerogels
 530 and cryogels via starch source and process parameter. *Carbohydrate Polymers*, 255,
 531 117344. <https://doi.org/10.1016/j.carbpol.2020.117344>

532
 533

534 **Caption of Figures**

535

536 Figure 1. Water vapor adsorption isotherms of cryogels and aerogels prepared from 5% (w/w)
537 cellulose solution (see density and porosity values in Table 2) and microcrystalline cellulose.
538 Error bars are not visible since smaller than the symbol size.

539

540 Figure 2. Water (A) and oil (B) absorbed by cryogels and aerogels prepared from cellulose
541 solutions containing 3, 4, 5% (w/w) cellulose. The symbols are the same for both figures. The
542 dashed lines are given to guide the eyes.

543

544 Figure 3. Maximum water and oil absorption capacity of cryogels and aerogels prepared from
545 cellulose solutions containing 3, 4, 5% (w/w) cellulose as a function of material porosity. The
546 dashed line is the least square approximation with $R^2 = 0.96$.

547

548 Figure 4. Firmness of cryogels and aerogels prepared from cellulose solutions containing 3, 4,
549 5% (w/w) cellulose prior to and after water and oil absorption as a function of porosity. The
550 dashed lines are added as a guide for eyes.

551

552

553 **Caption of Tables**

554

555 Table 1. Visual appearance and SEM microstructure of cryogels and aerogels prepared from
556 cellulose solutions containing 3, 4, 5% (w/w) cellulose.

557

558 Table 2. Volume variation, bulk density, porosity, pore volume, BET-specific surface area, and
559 firmness of cryogels and aerogels prepared from cellulose solutions containing 3, 4, 5% (w/w)
560 cellulose.

561

562 **Caption of Appendix Figures**

563

564 Figure A1. Water vapor adsorption isotherms of cryogels and aerogels prepared from cellulose
565 solutions containing 3 (A) and 4% (w/w) (B) cellulose (see density and porosity values in Table
566 2), and microcrystalline cellulose. Error bars are not visible since smaller than the symbol size.

567

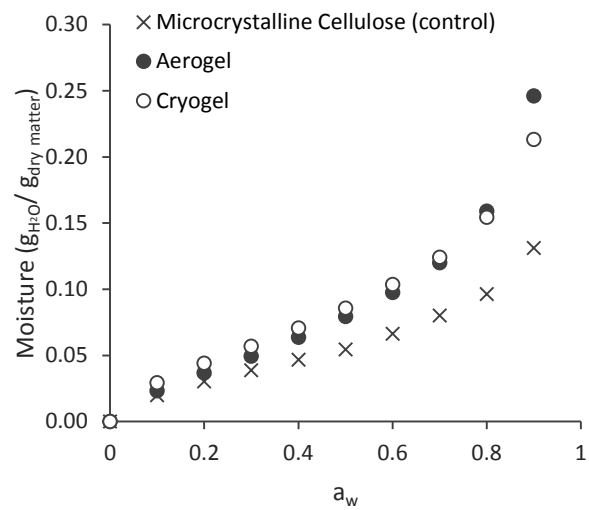


Figure 1

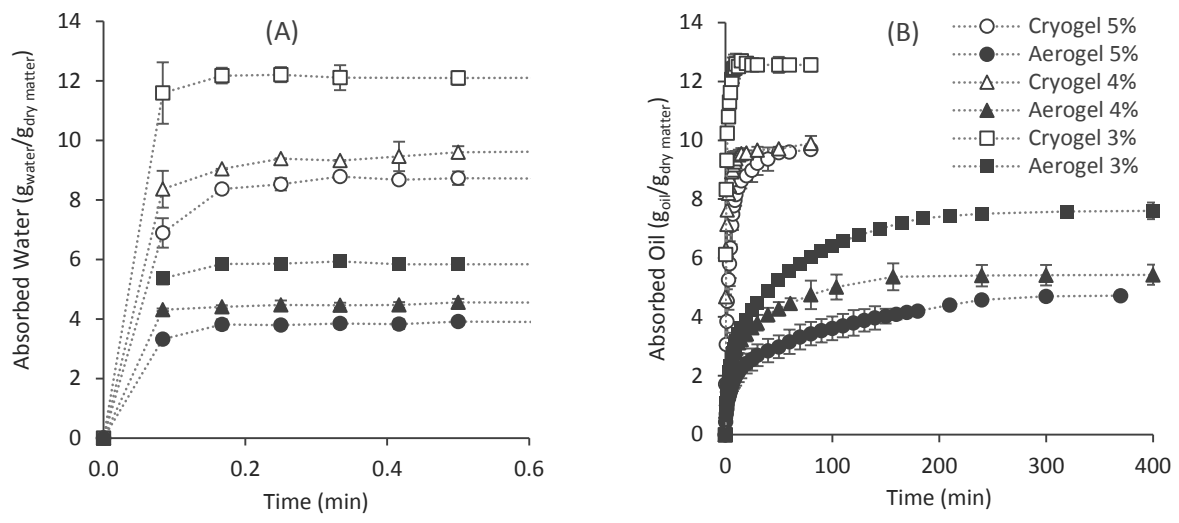


Figure 2

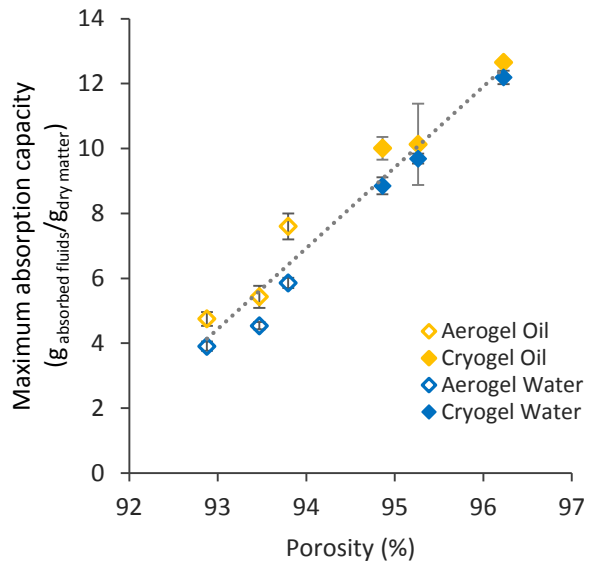


Figure 3

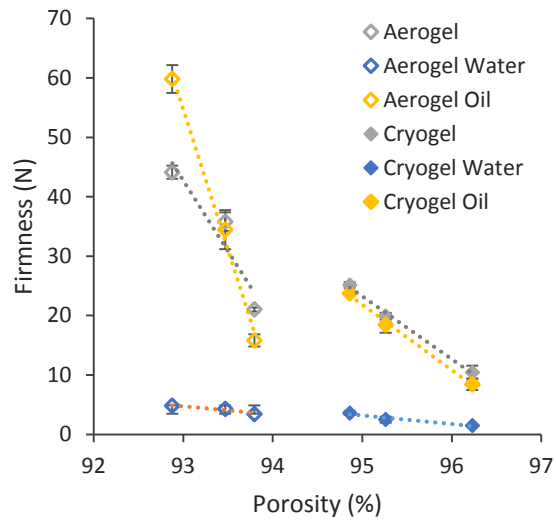


Figure 4

Declaration of interests

The authors declare that they have no known competing financial interests or personal relationships that could have appeared to influence the work reported in this paper.

The authors declare the following financial interests/personal relationships which may be considered as potential competing interests:

Signed by the corresponding author on behalf of all authors

Stella Placante

Udine, 15/12/2022

Author contributions

Francesco Ciuffarin: Methodology, Investigation, Formal analysis, Data curation, Visualization, Writing - original draft;

Marion Negreier: Methodology, Investigation, Writing - review & editing;


Plazzotta Stella: Conceptualization, Methodology, Investigation, Data curation, Visualization, Writing - review & editing;

Michele Libralato: Methodology, Writing - review & editing;

Sonia Calligaris: Conceptualization, Methodology, Writing - review & editing;

Tatiana Budtova: Conceptualization, Writing - review & editing, Funding acquisition, Supervision;

Lara Manzocco: Conceptualization, Writing - review & editing, Funding acquisition, Supervision.



Click here to access/download
Supplementary Material
Figure A1.docx